Article ID: 1000-324X(2023)05-0583-06 **DOI:** 10.15541/jim20220632

Growth and Property of Ce^{3+}-doped $La_2CaB_{10}O_{19}$ Crystal

LI Yue, ZHANG Xuliang, JING Fangli, HU Zhanggui, WU Yicheng

(Tianjin Key Laboratory of Functional Crystal Materials, Institute of Functional Crystals, School of Materials Science and Engineering, Tianjin University of Technology, Tianjin 300384, China)

Abstract: Besides its application as nonlinear optical devices, $La_2CaB_{10}O_{19}$ (LCB) crystal has been extensively studied as a host crystal due to excellent properties. Nevertheless, rare-earth (RE) ions doped LCB crystals for ultraviolet (UV) lasers have not been studied yet. In this work, Ce^{3+} doped $La_2CaB_{10}O_{19}$ (Ce^{3+}:LCB) crystal with the size of 40 mm×21 mm×6 mm was grown by top-seeded solution growth (TSSG) method. Its lattice parameters are slightly different from that of the LCB crystal, and its X-ray rocking curve indicates that the Ce^{3+}:LCB is of high crystalline quality. Transmittance spectrum and UV absorption spectrum measured at room temperature show intense absorption in the ranges of 200−288 nm and 305−330 nm,and Sellmeier equations for the refractive indices were determined by least-squares method. The excitation and fluorescence spectra show that there are two broad excitation peaks at 280 nm and 316 nm, corresponding to transitions of Ce^{3+} ions from 4f to 5d. Four emission peaks were obtained at 290, 304, 331, and 355 nm, which correspond to transitions from 5d state to $^2F_{5/2}$ state and $^2F_{7/2}$ state. Ce^{3+}:LCB crystal exhibits high thermal conductivity (6.45 W/(m·K)) at 300 K, and keeps good thermal stability with the increase of temperatures. Its thermal expansion coefficients and lattice parameters of *c* direction linearly enlarge from 2.94×10^{-6} /K and 0.91240 nm to 5.3×10^{-5} /K and 0.91246 nm in the temperature range from 358 K to 773 K, respectively. These results demonstrate that Ce^{3+}:LCB crystal has excellent optical properties and good thermal stability, which is conducive to its application for UV lasers.

Key words: Ce^{3+} doped $La_2CaB_{10}O_{19}$ crystal; optical property; thermal stability

$La_2CaB_{10}O_{19}$ (LCB) crystal has a large effective nonlinear optical coefficient (1.05 pm/V), moderate birefringence (0.053 at 1064 nm), high laser damage threshold (11.5 GW/cm^2), wide transmittance range (173–3000 nm), good thermal and mechanical properties[1-5]. Besides its application for laser frequency conversion, LCB has been proved a good host crystal, because La^{3+} ions in LCB crystal can be substituted by rare-earth (RE) ions, including Nd^{3+}, Sm^{3+}, Pr^{3+}, Yb^{3+}, Tb^{3+} and Er^{3+}[6-11]. These RE doped LCB crystals exhibit excellent optical and thermal properties, which illustrate that RE doped LCB crystals may be promising laser materials. For example, green laser radiation with the output of 26.64 mW were obtained by self-frequency doubling using a Nd^{3+}:LCB crystal[12].

On the other hand, Ce^{3+} doped laser crystals have been widely used in efficient and convenient all-solid-state ultraviolet (UV) lasers. It is reported that the main emission bands of Ce^{3+} ions in strong electronegativity fluoride and oxide matrix materials mainly locate in the UV range[13-18]. Since La^{3+} ions in a LCB crystal are surrounded by ten O^{2-} ions, the main fluorescence bands of Ce^{3+}:LCB crystal may occur in the UV region. To our knowledge, the optical and thermal properties of Ce^{3+} doped $La_2CaB_{10}O_{19}$ (Ce^{3+}:LCB) crystal have not been reported yet. Thus, it is an essential work to explore the optical and thermal properties of the Ce^{3+}:LCB crystal.

In this work, Ce^{3+}:LCB crystal has been grown by the top-seeded solution growth (TSSG) method. The XRD pattern and X-ray rocking curve of (010) face were collected. The transmittance, absorption, excitation, emission and radioluminescence spectra were studied at room temperature. Sellmeier equations for the refractive indices were calculated. Thermal conductivity, thermal

Received date: 2022-10-26; **Revised date:** 2022-12-05; **Published online:** 2023-02-13
Foundation item: National Natural Science Foundation of China (92163207, 51872198, 51890860, 51890865)
Biography: LI Yue (1993–), female, PhD candidate. E-mail: munchencindy171@163.com
李 悦(1993–), 女, 博士研究生. E-mail: munchencindy171@163.com
Corresponding author: JING Fangli, associate professor. E-mail: fljing@email.tjut.edu.cn
景芳丽, 副教授. E-mail: fljing@email.tjut.edu.cn

diffusivity and thermal expansivity of Ce^{3+}:LCB crystal were investigated. All of the above results demonstrate that Ce^{3+}:LCB crystal is promising for the lasing device in the UV range.

1 Experimental

1.1 Crystal growth

Ce^{3+}:LCB crystal, as large as 40 mm×21 mm×6 mm (Fig. 1(a)), was grown by TSSG method in a Li_2O-CaO-B_2O_3 flux system. The molar ratio of Ce_2O_3, La_2O_3, $CaCO_3$, Li_2CO_3 and H_3BO_3 was 0.03 : 0.97 : 2.00 : 2.30 : 28.00. The ground mixture was slowly heated and sintered at 950 ℃ for 20 h. Then, the charge materials were placed in a platinum crucible with a diameter of 60 mm and melted at 1020 ℃. The charge materials were transferred into a one-zone Kanthal A1 resistance furnace with an accurate Eurotherm controller after cooling. After transferred into a resistance heated furnace, Ce^{3+}:LCB crystal was grown by TSSG. The [110]-oriented seed was slowly dipped into the melting solution and kept rotating at 30 r/min in the whole growth. The melting solution was cooled at the rate of 1 ℃/d during the first 10 d and 1.5 ℃/d till the growth end. After about 30 d, the crystal was slowly pulled out of the solution and cooled down to the room temperature within one week with the initial cooling rate of 10 ℃/d. The grown crystal was cut and polished into dimensions of 10 mm×6 mm×1 mm with (010) surface (Fig. 1(b)).

1.2 Spectra measurements

The concentration of Ce^{3+} ions in a grown Ce^{3+}:LCB crystal was determined by Thermo Fisher iCAP RQ inductively coupled plasma atomic emission spectrometry (ICP-AES). X-ray diffraction data was collected using a Rigaku SmartLab 9 kW diffractometer with monochromatized with CuKα1 radiation (λ=0.15406 nm). The lattice parameters of the Ce^{3+}:LCB crystal were collected by Bruker SMART APEX II 4K CCD diffractometer with MoKα radiation (λ=0.071073 nm). The transmittance and absorption spectra of Ce^{3+}:LCB crystal was collected by Hitachi U4100 UV-VIS-NIR spectrophotometer over the wavelength range from 200 nm to 500 nm at room temperature. The refractive index was measured by Wedel UV-VIS-IR SpectroMaster refractive index meter with mercury and helium lamps light sources. The excitation and emission spectra of Ce^{3+}:LCB crystal were obtained by Edinburgh Analysis Instruments FLS980 spectrophotometer with Xenon lamp light source in the range from 230 nm to 400 nm with a step width of 0.1 nm. The thermal conductivity and thermal diffusivity were measured by NETZSCH LFA 457 NanoFlash analyzer in the temperature range from 300 K to 773 K. The thermal expansion coefficient was measured by NETZSCH DIL 402 thermal mechanical analyzer in the temperature range from 358 K to 773 K.

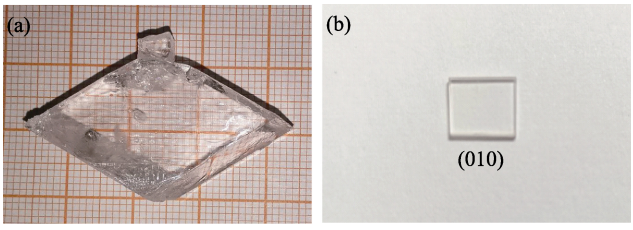

Fig. 1 Optical images of grown Ce^{3+}:LCB crystal
(a) As-grown Ce^{3+}:LCB crystal; (b) Cut and polished crystal with the (010) surface

2 Results and discussion

The concentration of Ce^{3+} ions in Ce^{3+}:LCB crystal was 1.05×10^{20} ions/cm^3. According to the effective segregation coefficient equation $K_{eff} = C/C_0$, where C is the dopant concentration in the crystal and C_0 is the dopant concentration in the mixture. The K_{eff} and molar ratio of Ce^{3+} to La^{3+} are calculated to be 0.58 and 1.74%, respectively.

Fig. 2(a) shows XRD pattern of an as-grown Ce^{3+}:LCB crystal with a standard LCB crystal. It reveals that the diffraction peaks of Ce^{3+}:LCB are consistent with that of LCB crystal. The lattice parameters of the Ce^{3+}:LCB crystal are a=1.1061 nm, b=0.6577 nm, c=0.9124 nm, α=γg=90°, β=91.5°, which are slightly different from those of the LCB crystal (a=1.1043 nm, b=0.6563 nm, c=0.9129 nm, α=γ=90°, β=91.5°). The Ce^{3+} ions are considered to substitute the La^{3+} ions due to the similar properties and radius of Ce^{3+} (0.1196 nm) and La^{3+} (0.1216 nm), leading to a slight change of the lattice after doping. Fig. 2(b) shows the X-ray rocking curve of (010) surface for the Ce^{3+}:LCB crystal. The full-width at half-maximum (FWHM) of (010) surface for Ce^{3+}:LCB crystal is 0.01473", indicating its very high quality.

The UV-Vis-NIR transmittance spectrum of a Ce^{3+}:LCB crystal is shown in Fig. 3(a). The transmittance exhibits a sharp decrease in the UV region due to characteristic absorption bands of Ce^{3+} ions. For the wavelength above 350 nm, the transmittance of Ce^{3+}:LCB crystal has almost constant value about 94%, indicating that its transparency in Vis and NIR regions is not obviously affected by Ce^{3+} ions doping.

Fig. 3(b) shows optical absorption spectrum of a Ce^{3+}:LCB crystal in the wavelength range from 200 nm to 500 nm. In the UV region, two main absorption peaks are

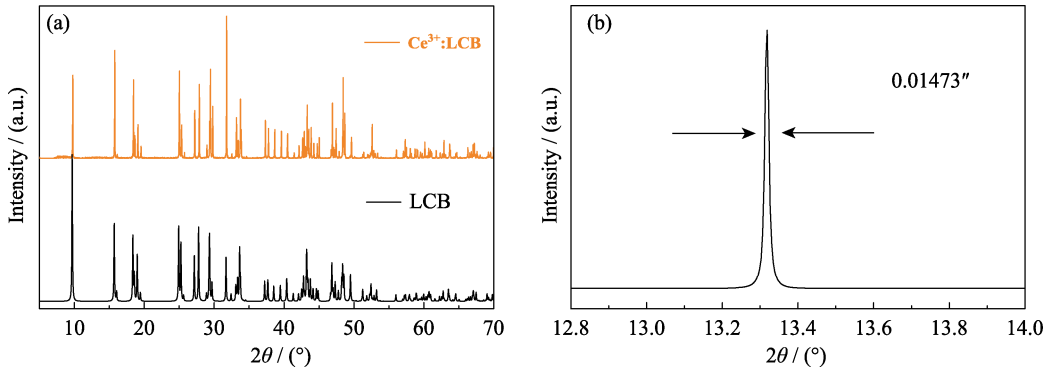

Fig. 2　X-ray diffraction analysis of Ce^{3+}:LCB crystal
(a) XRD patterns; (b) X-ray rocking curve on the (010) surface

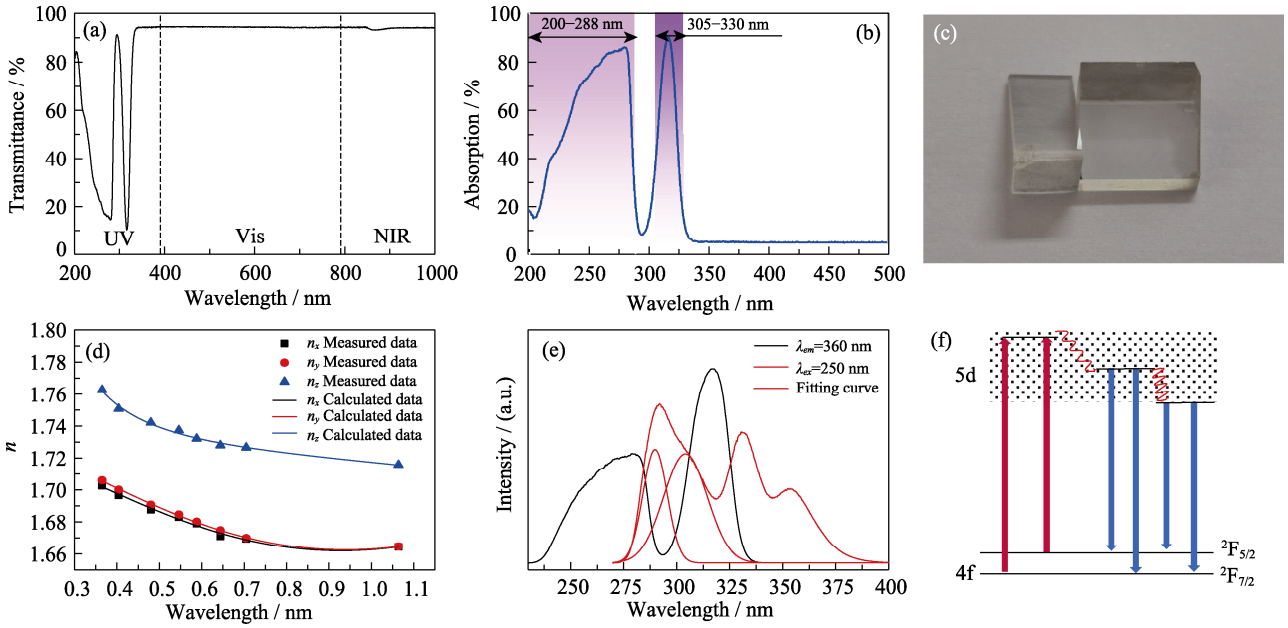

Fig. 3　Optical properties of Ce^{3+}:LCB crystal
(a) Transmittance spectrum at room temperature; (b) Absorption spectrum at room temperature; (c) Cut prisms; (d) Fitted refractive index curves; (e) Excitation and fluorescence spectra at room temperature; (f) Partial energy level diagram
Colorful figures are available on website

obtained at 280 and 316 nm, corresponding to typical characteristic absorption peaks of Ce^{3+} ions. Different from other trivalent rare-earth ions, Ce^{3+} ions in host crystals exhibit broad absorption bands. The absorption cross section (σ) can be calculated by Eq. (1):

$$\sigma = \frac{2.303 \times \mathrm{OD}(\lambda)}{N_0 L} \tag{1}$$

where $\mathrm{OD}(\lambda)$ is optical density function, N_0 is concentration of Ce^{3+} ions and L is optical length. The values of absorption cross section at 280 and 316 nm are 1.85×10^{-19} and 2.17×10^{-19} cm^2, respectively.

Since LCB is a biaxial crystal, the refractive indices of Ce^{3+}:LCB crystal was measured by two right-angle prisms with different light-pass surfaces. The orientations of the two prisms are similar to those of $La_2CaB_{10}O_{19}$ crystals, as reported in Ref. [19]. The cut prisms of Ce^{3+}:LCB crystal are shown in Fig. 3(c). Its refractive indices are obtained by improved Sellmeier equations:

$$n^2 = A + \frac{B}{\lambda^2 - C} - D \times \lambda^2 \tag{2}$$

where n is refractive index, λ is the incident wavelength and the constant of A, B, C, D can be obtained in terms of least-squares fit. The measured three principal refractive indices (n_x, n_y, n_z) are listed in Table 1. The n_x, n_y, n_z at other wavelengths can be calculated by Eq. (3):

$$\begin{aligned} n_x^2 &= 2.7721 + \frac{0.01827}{\lambda^2 - 0.00115} - 0.02863\lambda^2 \\ n_y^2 &= 2.75914 + \frac{0.02406}{\lambda^2 - 0.02041} - 0.01842\lambda^2 \\ n_z^2 &= 2.97889 + \frac{0.01127}{\lambda^2 - 0.04891} - 0.04124\lambda^2 \end{aligned} \tag{3}$$

Based on Sellmeier equations, refractive indices at UV regions can be calculated, which provides essential parameters of Ce^{3+}:LCB crystal for UV laser applications. Fig. 3(d) shows the fitted curves of three principal refractive indices. It can be seen that the Ce^{3+}:LCB

Table 1 Refractive indices of Ce^{3+}:LCB crystal

λ/μm	n_x	n_y	n_z
0.365	1.70260	1.70603	1.76262
0.404	1.69658	1.70012	1.75075
0.480	1.68758	1.69071	1.74215
0.546	1.68294	1.68464	1.73736
0.588	1.67904	1.68017	1.73216
0.644	1.67101	1.67477	1.72806
0.705	1.66936	1.66996	1.72663
1.064	1.66450	1.66470	1.71581

crystal belongs to a positive biaxial optical crystal with a birefringence Δn =0.051 at 1064 nm, which is close to that of LCB crystal (Δn = 0.053 at 1064 nm)[20]. These results indicate that the birefringence of the grown crystal is almost not affected by small amounts of RE ions doping.

Excitation and fluorescence spectra of Ce^{3+}:LCB crystal at 300 K are shown in Fig. 3(e). The excitation and fluorescence bands of Ce^{3+}:LCB crystal are broad, which is determined by parity-allowed electric dipole transitions 4f→5d. Two broad excitation bands are observed in the UV regions of 240–290 nm and 290–340 nm, which correspond to transitions from 4f ($^2F_{5/2}$ and $^2F_{7/2}$) ground states to 5d excited states. The fluorescence bands are inhomogeneously broadening. Four obvious emission bands are obtained at 290, 304, 331, and 353 nm by Gauss fitting, which correspond to transitions from 5d states to $^2F_{5/2}$ and $^2F_{7/2}$ states (Fig. 3(f)). The f-d transition energy of Ce^{3+} ions in the Ce^{3+}:LCB crystal is calculated to be 33557, 15783 cm^{-1}, lower than that of free Ce^{3+} ions (49340 cm^{-1})[21]. The separation between $^4F_{7/2}$ and $^4F_{5/2}$ states is 2134 cm^{-1}, which agrees well with the theoretical value of 2250 cm^{-1}[22]. It is worth to mention that main fluorescence range (280–380 nm) of Ce^{3+}:LCB crystal is located in the UV region due to the reduction of 5d states. The results can provide essential parameters of Ce^{3+}:LCB crystal for the application of UV lasers.

The temperature dependence of thermal conductivity and thermal diffusivity for Ce^{3+}:LCB crystal are shown in Fig. 4(a, b). Thermal conductivity and thermal diffusivity are 6.45 W/(m·K) and 1.76 mm^2/s at 300 K, respectively, and then gradually decrease to 2.254 W/(m·K) and 0.583 mm^2/s as the temperature rises to 773 K. Thermal conductivity and thermal diffusivity of Ce^{3+}:LCB crystal only decrease about 45% when temperature increases from 300 K to 423 K, less than those of Nd^{3+}-doped $LiLuF_4$ (Nd^{3+}:LLF) crystal (50%)[23]. Therefore, Ce^{3+}:LCB crystal exhibits better thermal stability and wider operational temperature range. The temperature dependence of thermal conductivity $k(T)$ is approximated by the polynomial:

$$k(T) = A_1T^3+B_1T^2+C_1T+D_1 \quad (4)$$

A_1, B_1, C_1, and D_1 coefficients for Ce^{3+}:LCB crystal are

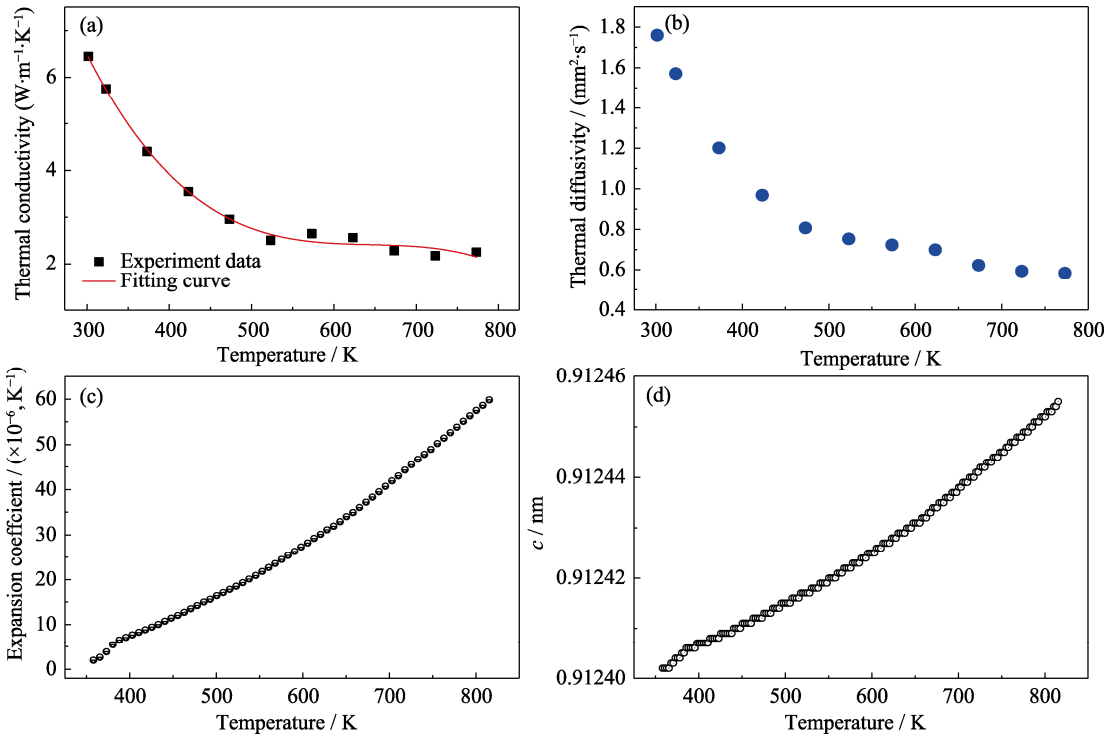

Fig. 4 Thermal property of Ce^{3+}:LCB crystal

(a) Temperature dependence of thermal conductivity; (b) Temperature dependence of thermal diffusivity along the [010] direction; (c) Thermal expansion coefficient; (d) Temperature dependence of lattice parameters along the *c* direction

calculated to be -9.67×10^{-8} W/(m·K^4), 1.87×10^{-4} W/(m·K^3), –0.12 W/(m·K^2) and 28.50 W/(m·K), respectively.

For Ce^{3+}:LCB crystal along the *c* direction, temperature-dependent thermal expansion coefficient and lattice parameters of *c* direction are shown in Fig. 4(c, d). The expansion coefficient and lattice parameter are 2.94×10^{-6} /K and 0.91240 nm at 358 K, and then linearly enlarged to 5.3×10^{-5} /K and 0.91246 nm at 773 K. The Ce^{3+}:LCB crystal with smaller lattice distortion tends to sustain a larger thermal shock under laser irradiation. These results demonstrate that Ce^{3+}:LCB crystal exhibits better thermal stability over a wider temperature, which benefits for its application for UV lasers.

3 Conclusions

In summary, Ce^{3+}:LCB crystals have been grown by TSSG method in Ca_2O-Li_2O-B_2O_3 flux system. The lattice parameters of Ce^{3+}:LCB are a=1.1061 nm, b= 0.6577 nm, c=0.9124 nm, $\alpha=\gamma$=90°, β=91.5°. The FWHM of X-ray rocking curve is 0.01473", indicating good crystalline quality of the grown Ce^{3+}:LCB crystal. The main absorption bands and excitation bands of Ce^{3+}:LCB crystal are located in 200–288 nm and 305–330 nm regions. Four emission peaks are obtained at 290, 304, 331, and 353 nm, corresponding to transitions from 5d states to $^2F_{5/2}$ and $^2F_{7/2}$ states. The values of thermal conductivity and thermal diffusivity are 6.45 W/(m·K) and 1.76 mm^2/s at 300 K, respectively. Furthermore, the thermal stability of Ce^{3+}:LCB crystal is slightly higher than that of Nd^{3+}:LLF crystal. The lattice parameter of Ce^{3+}:LCB crystal along *c* direction extremely slowly increases from 0.91240 to 0.91246 nm with increasing the temperature from 358 K to 773 K, exhibiting good temperature stability. With excellent optical property and enhanced thermal stability, Ce^{3+}:LCB crystal is suggested to be a potential candidate for high performance and high reliability UV laser materials.

References:

[1] WU Y C, FU P Z, ZHENG F, *et al.* Growth of a nonlinear optical crystal $La_2CaB_{10}O_{19}$ (LCB). *Optical Materials*, 2003, **23(1/2):** 373.

[2] JING F L, WU Y C, FU P Z. Growth of $La_2CaB_{10}O_{19}$ single crystals from CaO-Li_2O-B_2O_3 flux. *Journal of Crystal Growth*, 2005, **285(1/2):** 270.

[3] JING F L, WU Y C, FU P Z. Growth of $La_2CaB_{10}O_{19}$ single crystals by top-seeded solution growth technique. *Journal of Crystal Growth*, 2006, **292(2):** 454.

[4] WU Y C, LIU J G, FU P Z, *et al.* A new lanthanum and calcium borate $La_2CaB_{10}O_{19}$. *Chemistry of Materials*, 2001, **13(3):** 753.

[5] WANG G L, LU J H, CUI D F, *et al.* Efficient second harmonic generation in a new nonlinear $La_2CaB_{10}O_{19}$ crystal. *Optics Communications*, 2002, **209(4/5/6):** 481.

[6] BRENIER A, WU Y, ZHANG J X, *et al.* Laser properties of the diode-pumped Nd^{3+}-doped $La_2CaB_{10}O_{19}$ crystal. *Journal of Applied Physics*, 2010, **108(9):** 093101.

[7] ZHANG X Y, WU Y, SHAN F X, *et al.* Growth and spectroscopic properties of Sm^{3+}-doped $La_2CaB_{10}O_{19}$ crystal. *Journal of Crystal Growth*, 2014, **399:** 39.

[8] ZU Y L, ZHANG J X, ZHENG F, *et al.* Growth and optical properties of Pr^{3+}: $La_2CaB_{10}O_{19}$ crystal. *Journal of Rare Earths*, 2009, **27(6):** 911.

[9] BRENIER A, WU Y, ZHANG J X, *et al.* Lasing Yb^{3+} in crystals with a wavelength dependence anisotropy displayed from $La_2CaB_{10}O_{19}$. *Applied Physics B*, 2012, **107:** 59.

[10] SHAN F X, FU Y, ZHANG G C, *et al.* Growth and spectroscopic properties of Tb^{3+} doped $La_2CaB_{10}O_{19}$ crystal. *Optical Materials*, 2015, **49:** 27.

[11] GUO R, WU Y C, FU P Z, *et al.* Optical transition probabilities of Er^{3+} ions in $La_2CaB_{10}O_{19}$ crystal. *Chemical Physics Letters*, 2005, **416(1/2/3):** 133.

[12] ZHANG J X, HAN L, WU Y, *et al.* Multiple-wavelength lasing by multiform self-frequency conversion in Nd^{3+}-doped $La_2CaB_{10}O_{19}$ crystals. *Applied Physics B*, 2011, **103:** 853.

[13] DUBINSKII M A, SCHEPLER K L, SEMASHKO V V, *et al.* Spectroscopic analogy approach in selective search for new Ce^{3+}-activated all-solid-state tunable ultraviolet laser materials. *Journal of Modern Optics*, 1998, **45(2):** 221.

[14] YAMAGA M, IMAI T, MIYAIRI H, *et al.* Substitutional disorder and optical spectroscopy of Ce^{3+}-doped $CaNaYF_6$ crystals. *Journal of Physics: Condensed Matter*, 2001, **13:** 753.

[15] LIU Z L, SHIMAMURA K, NAKONO K, *et al.* Direct generation of 27-mJ, 309-nm pulses from a Ce^{3+}:$LiLuF_4$ oscillator using a large-size Ce^{3+}: $LiLuF_4$ crystal. *Japanese Journal of Applied Physics*, 2000, **39:** 88.

[16] SRIVASTAVA A M, SETLUR A A, COMANZO H A, *et al.* Optical spectroscopy and thermal quenching of the Ce^{3+} luminescence in yttrium oxysulfate $Y_2O_2[SO_4]$. *Optical Materials*, 2008, **30(10):** 1499.

[17] MORI M, NAKAUCHI D, OKADA G, *et al.* Scintillation and optical properties of Ce^{3+}-doped $CaGdAl_3O_7$ single crystals. *Journal of Luminescence*, 2017, **186:** 93.

[18] WU Y T, REN G H. Crystal growth, structure, optical and scintillation properties of Ce^{3+}-doped $Tb_{2.2}Lu_{0.8}Al_5O_{12}$ single crystals. *CrystEngComm*, 2013, **20:** 4153.

[19] ZHANG X L, LI Y, JING F L, *et al.* Studies on the crystal growth and characterization of large size Sr:LCB single crystals. *Crystals*, 2022, **12(4):** 442.

[20] ZHANG J X, WANG L R, WU Y, *et al.* High-efficiency third harmonic generation at 355 nm based on $La_2CaB_{10}O_{19}$. *Optics Express*, 2011, **19(18):** 16722.

[21] REISFELD R, HORMODALY J, BARNETT B. Ce^{3+} as a probe of the crystal field and the nature of the impuruty-ligand bond in borate and phosphate glasses. *Chemical Physics Letters*, 1972, **17(2):** 248.

[22] REISFELD R, JRGENSEN J K. Laser and Excited State of Rare Earths. New York: Springer, 1977.

[23] ZHANG P X, WAN Y B, YIN J G, *et al.* Spectroscopic, thermal and laser characteristics of Nd:$LiLuF_4$ for 1314 nm laser. *Laser Physics Letters*, 2014, **11(11):** 115803.

铈掺杂硼酸钙镧晶体的生长与性能研究

李 悦, 张旭良, 景芳丽, 胡章贵, 吴以成

(天津理工大学 材料科学与工程学院, 功能晶体研究院, 天津市功能晶体材料重点实验室, 天津 300384)

摘 要: 硼酸钙镧晶体是一种激光基质晶体, 以其优秀的物理特性而受到广泛关注。稀土离子掺杂的硼酸钙镧晶体在紫外激光器领域的研究尚不多见。本研究采用顶部籽晶法成功生长出尺寸为 40 mm×21 mm×6 mm 的铈掺杂硼酸钙镧晶体。研究了铈掺杂硼酸钙镧晶体室温光谱性质, 测量了室温下其透过光谱以及紫外−吸收光谱, 发现铈离子掺杂导致晶体在 200~288 nm 以及 305~330 nm 紫外波段吸收较强。测试了室温下铈掺杂硼酸钙镧晶体的激发光谱, 并且利用波长 260 nm 的连续光激发得到发射光谱, 发现主要发射带中心波长位于 290, 304, 331 和 353 nm 处, 对应于铈离子 5d 态到 $^2F_{5/2}$ 和 $^2F_{7/2}$ 态的跃迁。对铈掺杂硼酸钙镧晶体的热学性质进行了研究, 发现其在 300 K 下具有较高的热导率(6.45 W/(m·K)), 且随着温度升高保持良好的热稳定性。358 K 条件下, 热膨胀系数及 *c* 方向的晶格常数分别为 2.94×10^{-6} /K 和 0.91240 nm, 随着温度升高至 773 K，线性增加到 5.3×10^{-5} /K 和 0.91246 nm。研究结果表明：铈掺杂硼酸钙镧晶体具有良好的光学性能和热稳定性, 适合应用于紫外激光领域。

关 键 词: 铈掺杂硼酸钙镧晶体；光学性能；热稳定性

中图分类号: O78 **文献标志码:** A